Inorganica Chimica Acta 559 (2024) 121790

Contents lists available at ScienceDirect

Inorganica Chimica Acta

journal homepage: www.elsevier.com/locate/ica

Spontaneous transmetalation at the ZnPc/Al(100) interface

Guido Fratesi [a,*], Daniele Paoloni [b,*], Luca Persichetti [c,*], Luca Camilli [c], Antonio Caporale [c], Anu Baby [d,1], Dean Cvetko [e,f,g], Gregor Kladnik [e,g], Alberto Morgante [g,h], Alessandro Ruocco [b]

[a] Physics Department "Aldo Pontremoli", University of Milan, via Celoria 16, 20133 Milano, Italy
[b] Dipartimento di Scienze, Università degli Studi Roma Tre, Via della Vasca Navale 84, 00146 Rome, Italy
[c] Dipartimento di Fisica, Università di Roma "Tor Vergata", Via Della Ricerca Scientifica, 1-00133 Rome, Italy
[d] Department of Materials Science, University of Milano-Bicocca, 20125 Milano, Italy
[e] University of Ljubljana, Faculty of Mathematics and Physics, Ljubljana SI-1000, Slovenia
[f] Institute J. Stefan, Ljubljana SI-1000, Slovenia
[g] Laboratorio TASC CNR-IOM, Trieste 34127, Italy
[h] Physics Department, University of Trieste, Trieste 34127, Italy

ARTICLE INFO

Keywords:
Transmetalation
Surface reaction
Aluminium-phthalocyanine
Electronic and magnetic properties
Scanning tunneling microscopy

ABSTRACT

Metal-phthalocyanines (MPcs) are a class of organic macrocycles that have received much attention for their potential use in various applications, including molecular electronics. In recent years, the on-surface synthesis of different MPcs has been demonstrated via deposition of atomic species, sample heating and scanning tunneling microscopy (STM) manipulation. However, the spontaneous substitution of the central metal atom with a substrate one, known as transmetalation, remains a less explored process. Here, we study the transmetalation of ZnPc on Al(100) using a combination of STM and density functional theory (DFT) computations. Previously published X-ray photoelectron spectroscopy (XPS) data indicate the absence of Zn atoms from the interface, while our STM images show that a central atom is still present. This suggests that the transmetalation process occurs spontaneously for all ZnPc molecules. Our DFT calculations reveal that the transmetalation of Zn with Al releases 2 eV per molecule, providing thermodynamic evidence for the process. The on-surface synthesized aluminium phthalocyanine (AlPc) molecules are stabilised by the formation of a bond between the central metal atom and the substrate, similar to that found in chloroaluminium phthalocyanine (ClAlPc), with the consequent suppresion of the paramagnetism of free AlPc.

1. Introduction

Phthalocyanines (Pcs) are organic semiconductors composed by a macrocycle with 4 isoindolic groups bonded together by 4 aza-bridge nitrogen atoms. This macrocycle has 16 reactive sites and its center can host over 70 distinct metal ions [1]. The presence of a different central atom affects the symmetry of the molecule [2], and, in turn, its electronic structure [3] and magnetic properties [4]. For example, transition metal Pcs have D_{4h} symmetry and the position of their b_{1g} electronic level changes as a function of the central atom [3]. Conversely, the metal-free H_2Pc, a molecule with two hydrogen atoms in the center, has D_{2h} symmetry [2]. Moreover, when the central atom has a large atomic number (PbPc and SnPc), it is located outside the molecular plane (C_{4v}) [2]. Similar to porphyrins, if the central atom is not divalent, an axial substituent is necessary to stabilise the molecule [5,1] (for example, ClAlPc and TiOPc), thus filling the bonds of the central atom.

Up to now different Pcs have been grown on diverse substrates (either metallic or non metallic) giving rise to different interface properties [6]. Some substrates, such as HOPG [7,8], do not affect the Pc electronic structure, while on others, for instance Ag(111) [9], some charge is transferred from the substrate to interface molecules with the formation of hybrid orbitals. An interesting aspect of the growth of Pc on specific substrates is the possibility to exploit adsorbate–surface and adsorbate–adsorbate interactions to perform the on-surface synthesis of new molecules [10]. For example, FePc can be obtained on Pb(111) [11] and Ag(111) [12] by depositing iron atoms on a H_2Pc sub-monolayer (metalation). The replacement of the central atoms can even be

* Corresponding authors.
E-mail addresses: guido.fratesi@fisica.unimi.it (G. Fratesi), daniele.paoloni@uniroma3.it (D. Paoloni), luca.persichetti@uniroma2.it (L. Persichetti).
[1] Now at: STMicroelectronics, Via Tolomeo 1, 20010 Cornaredo, Italy.

https://doi.org/10.1016/j.ica.2023.121790
Received 5 July 2023; Received in revised form 27 September 2023; Accepted 28 September 2023
Available online 2 October 2023

achieved by a scanning tunneling microscope (STM) tip, which can trigger, for example, the inclusion of Pb atoms into H_2Pc on Ag(111) [13] or the removing of the central atom from the PbPc on Ag(111) [14] (demetalation). Moreover, self-metalation of H_2Pc on Ag(110) and Cu (111) has been observed [15,16], consisting of the spontaneous replacement of the two hydrogen atoms with a substrate atom. When the central metal atom of the deposited molecule is replaced by another atom from the substrate, the process is called transmetalation. Transmetalation has been reported for CoPc [17] and some porphyrins [18,19] on copper. However, this process is one of the less studied among phthalocyanines and porphyrins surface reactions [10,20] and it generally requires high temperature to be activated: the complete transmetalation of CoPc on copper is only obtained at 300 °C [17], thus motivating the investigation of conditions for lower temperature activation, which could enhance our fundamental understanding of the process by revealing the favorable conditions for its occurrence.

In this work we analyse transmetalation at the ZnPc/Al(100) interface. It has been shown that the bulk growth of Pc on Al(100) is disordered [21]. This phenomenon may be attributed to the significant interaction between the molecules of the first layer and the Al(100) surface, consisting in a charge transfer from the substrate to the Pc lowest unoccupied molecular orbital (LUMO) [22]. Since the interaction between the molecule and the substrate is strong, the reorganization of the adsorbed molecules is very low [23]. Additionally, due to the altered electronic structure of the interface molecules, second layer molecules are unable to stack on them [7]. Therefore, the second layer molecules form columns in any direction parallel to the surface, thus causing a significant disorder [21] in their azimuthal orientation. In addition to charge transfer, the Pc/Al(100) interface is characterized by the spontaneous loss of all the zinc atoms of the ZnPc at room temperature, while a subsequent annealing to 160 °C triggers the diffusion of zinc atoms into the crystal [23]. Up to now, however, the final state of the molecule after the demetalation process remains unclear, whether this being a metal-free Pc without a central atom or the AlPc. AlPc, which is of interest for its magnetic properties [24], is an air unstable molecule since it includes a trivalent atom in a macrocycle with −2 oxidation state. Given the instability of the free molecule, on-surface synthesis approaches have been proposed to produce AlPc via reactions occurring at the interface. In particular, after the deposition of Al atoms on H_2Pc/Au (111), some of the H_2Pcs spontaneously metalate, forming AlPc [24]. Alternatively, other authors found that the deposition of ClAlPc on Pb (100) and the subsequent annealing to 200 °C lead to chlorine removal from the molecule [25].

Here, we combine density functional theory (DFT) and STM to determine the resulting molecule after the adsorption of ZnPc on Al (100). The results are compatible and rationalized with the published X-ray photoelectron spectroscopy (XPS) results in literature [23]. We demonstrate that ZnPc transmetalates resulting in the synthesis of the AlPc. Differently from the transmetalation processes observed on copper [17], this process happens spontaneously at room temperature for all the molecules. We suggest that the central atom, since it is trivalent inside a Pc ring, can bond to the substrate, making the transmetalation and the synthesis of AlPc possible.

2. Methods

We perform DFT simulations with the Perdew Burke Ernzerhof (PBE) exchange correlation functional, [26] including dispersion interactions by the Grimme D3 method [27]. Selected configurations are also investigated by the hybrid functional proposed by Heyd, Scuseria, and Ernzerhof (HSE) [28,29]. Calculations are based on plane waves and ultrasoft pseudopotentials as implemented in QuantumESPRESSO [30,31]. We adopt pseudopotentials from PSlibrary [32] with plane wave cutoffs of 46 and 326 Ry for the wavefunction and density, respectively. We take the theoretical Al lattice parameter (4.038 Å) and simulate the Al(100) surface by the slab model, including 3, 5, and 10 Al layers for a preliminary scan of the geometries, their refinement, and post-relaxation calculation of the electronic density of states, respectively. The Brillouin zone of the 5×5 surface unit cell is sampled by a 4×4 k-point mesh. Preliminary geometry scans adopt a Methfessel-Paxton smearing of 0.02 Ry, which is reduced to 0.005 Ry for the subsequent refinement. Additional calculations at lower broadening (0.001 Ry, see below) have been performed to verify the independence of the results on this parameter. Constant-height STM images are simulated by the Tersoff-Hamann method as the local density of states integrated between the applied bias (1 V) and the Fermi energy.

An Al(100) single-crystal was cleaned by several cycles of Ar^+ sputtering at 3 kV at 2×10^{-5} mbar followed by annealing to 420 °C, performed using a radiative heater. ZnPc molecules, purity 95%, have been purchased from Sigma–Aldrich and purified in ultrahigh-vacuum (UHV) for many hours at 200 °C. A nominal coverage of 0.6 Å of ZnPc molecules is sublimated with an evaporation rate of 0.33 Å/min, determined using a quartz crystal microbalance. The substrate temperature is kept at room temperature during the evaporation. After a first set of measurements, the sample was heated at 160 °C for 2 min to make zinc atoms diffuse into the crystal [23]. Isolated molecules were imaged by STM using W tips at a temperature of 9 K in UHV (base pressure $<5 \times 10^{-11}$ mbar) using a Scienta Omicron Infinity System. STM images have been processed using the Gwyddion software by leveling the data with the subtraction of a background plane and by applying a Fourier filter. Unfiltered images are reported as supplementary information.

3. Theoretical results

3.1. Adsorption configuration

To study the final state of ZnPcs deposited on Al(100), we compute the formation energy of different Pc configurations. Since the presence of H_2Pc has been excluded by XPS [23], we study ZnPc, AlPc and a Pc ring where the Zn atom is extracted from the molecule and dissolved in the Al bulk, leaving a vacancy in the molecule before structural optimization; we indicate such configuration as ·Pc. First, we estimate the azimuthal rotation of the molecules. Given the results of the diffraction data presented in the literature [23], we consider adsorption in a square 5×5 Al(100) surface unit cell. Even if other reconstructions, such as the c(10 × 10), are compatible with the experimental data, the 5×5 reconstruction represents the smallest possible unit cell into which the molecule can fit on the Al(100) surface hence appearing likely to occur at monolayer completion. Since the cell side (14.28 Å) is shorter than the molecule diameter (≈ 15 Å), this implies a rotation of the molecules around an axis orthogonal to the surface plane. As a first step we estimate the azimuthal angle ϕ of such rotation by optimizing the structure of a square arrangement of free-standing ZnPc molecules having the same lattice vectors as Al(100)-5 × 5: a value $\phi = 26°$ is obtained. That model is then transferred to the surface and, upon further optimization, the same value ϕ is obtained for adsorbed ZnPc and AlPc. See for example AlPc in Fig. 1(a).

We estimate the adsorption energy of ZnPc and AlPc molecules following standard practice as

$$E^{\mathrm{ads}} = E^{\mathrm{tot}}_{\mathrm{mol/surf}} - E^{\mathrm{tot(g)}}_{\mathrm{mol}} - E^{\mathrm{tot}}_{\mathrm{surf}}, \tag{1}$$

where on the right hand side we have the total energies of the combined system and isolated molecule and surface. The values are reported in Table 1, for the molecule centered on a surface top or hollow site.

One can see that the adsorption energy of the two molecules is comparable, being only 0.2 −0.4 eV larger for AlPc. ZnPc exhibits a small preference towards the hollow site, whereas AlPc is more stable on-top. These energies include an intermolecular contribution for which an estimate of −0.14 eV can be extracted by comparing E^{ads} for AlPc in a more diluted 6 × 6 unit cell. For the sake of the forthcoming discussion, we further report the adsorption energy of AlPc on two cases: one atop of

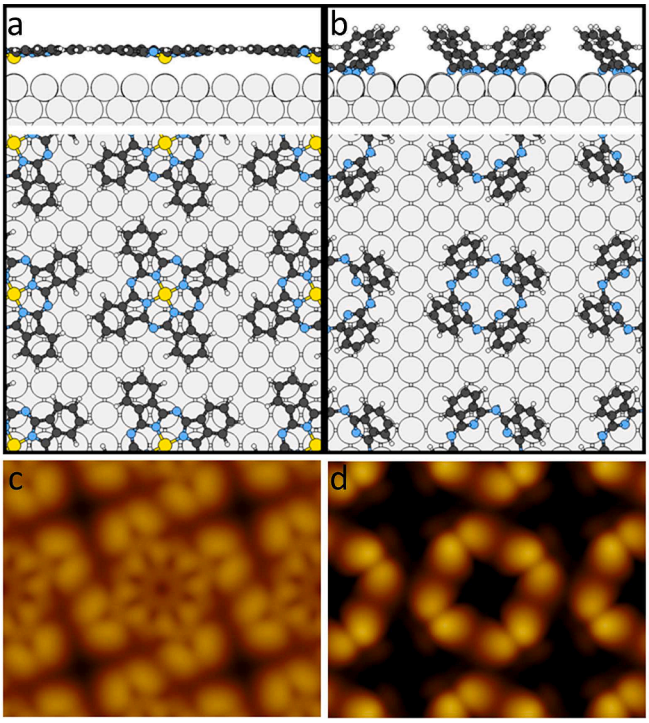

Fig. 1. Top and side views of the structure of (a) AlPc in a top site and (b) ·Pc in a hollow site. Dark gray, blue, small white, and yellow circles indicate C, N, H, and Al atoms from the molecules, respectively. Large circles are for surface Al atoms. The structures of ZnPc and that of ·Pc in a top site, resulting in the extraction of a surface atom, are analogous to the one in panel (a). Panels (c) and (d) report simulated STM images at $V = -1$ V of AlPc in a top site and ·Pc in a hollow site, respectively.

Table 1
Adsorption energy of ZnPc and AlPc on Al(100) by DFT.

Molecule	Site	E^{ads} (eV)
ZnPc	hollow	−2.13
ZnPc	top	−2.10
AlPc	hollow	−2.35
AlPc	top	−2.51
AlPc	Zn in Al(100)	−2.51
AlPc	Zn adatom	−2.44

a Zn atom substitutional in the first layer of Al(100), and one above a Zn adatom on Al(100). The corresponding energies are similar to that of the top site.

To address the stability of the molecules on the surface, and the energetics of the transmetalation process, we further compute the formation energy of the structures starting from gas phase ZnPc and clean Al(100) (Table 2). Following the observed migration of Zn to bulk Al, we take this as the reservoir of Zn atoms and define the formation energy as:

$$E^{form}_{mol/surf} = E^{tot}_{mol/surf} - E^{tot}_{ZnPc} - E^{tot}_{Al(100)} - N_{Al}\mu_{Al} - N_{Zn}\mu_{Zn}. \quad (2)$$

Here, the reference energies are the total energy of gas phase ZnPc (E^{tot}_{ZnPc}), that of the clean 5 × 5 slab ($E^{tot}_{Al(100)}$), the energy per atom of bulk Al (μ_{Al}), and the energy of a Zn atom embedded in Al (μ_{Zn}). The latter is computed with a 4 × 4 × 4 Al supercell, that provides convergent results, as: $\mu_{Zn} = E^{tot}_{ZnAl_{63}} - 63\mu_{Al}$. We refer to the extra number of Al and Zn atoms with respect to ZnPc and clean Al(100), as N_{Al} and N_{Zn}, respectively. Clearly, for ZnPc adsorbed intact, $N_{Al} = N_{Zn} = 0$ so that $E^{form} = E^{ads}$ as given above.

Table 2
Formation energy of ZnPc, ·Pc, and AlPc. The adsorption of ·Pc in the hollow site leads to a distortion of the molecule to bind to the surface through the central N atoms. The adsorption of ·Pc in the top site leads to the metalation of the molecule, forming an AlPc over a vacancy. The last two rows correspond to an AlPc on top of a Zn atom substitutional in the first layer of Al(100) and AlPc above a Zn adatom on Al(100).

Molecule	Configuration	E_{form} (eV)
ZnPc	hollow	−2.13
ZnPc	top	−2.10
·Pc	hollow	−2.46
·Pc	top	−3.37
AlPc	hollow	−4.06
AlPc	top	−4.22
AlPc	Zn in Al(100)	−4.26
AlPc	Zn adatom	−4.06

In this analysis we include demetalated (·Pc) species. These are significantly less stable in the gas phase, where it costs 6.2 eV to remove a Zn atom from ZnPc, and 10.1 eV to remove Al from AlPc. Nevertheless, these can interact so strongly with the surface to yield a more favorable configuration than adsorbed ZnPc. We find that the on top adsorption leads to the incorporation of an Al atom from the surface in the ·Pc, forming AlPc (alike the AlPc case of Fig. 1a), so that ·Pc/top becomes AlPc on an Al(100) surface vacancy. This process happens without any barrier, testifying the easiness of the metal exchange process. Instead, in the hollow site, ·Pc distorts so as to bind to the surface through the central N atoms (Fig. 1b). The two final configurations exhibit evident morphological differences and can be clearly distinguished by STM, as demonstrated by the reported STM simulated images in Figs. 1c and 1d. We verified that this distortion does not depend on the intermolecular packing, as the same is also computed for a larger 6 × 6 unit cell. As previously mentioned, the 5 × 5 is not the only unit cell compatible with the diffraction data [23]. The calculations just reported show that in any case the 5 × 5 and the 6 × 6 reconstructions, which differ in packing and surface density, do not give rise to different morphology of adsorbed molecules nor to significant changes of the adsorption energy per molecule. In other words, the in-plane intermolecular interaction does not seem to influence the molecule–substrate bond. Therefore, the reported results should be valid even if the real reconstruction was not the 5 × 5 (which being denser optimises the surface energy) but one with a lower surface density such as the c(10 × 10).

Eventually, the formation energy largely favors AlPc, so that the exchange of the Zn atom for a bulk Al one releases ≈ 2 eV per molecule.

The energy gain for the Zn-Al exchange in ZnPc/Al(100) can be understood if one compares the binding energy of Zn and Al atoms to bulk Al and to the center of a Pc molecule. Indeed, we find that exchanging a bulk Al atom with a free Zn atom costs ≈ 2 eV, an energy that is more than balanced by the energy gain of exchanging a Zn atom in the free molecule with a free Al one (≈ 4 eV difference). With respect to these values, the difference in adsorption energy (0.2-0.4 eV stronger for AlPc than ZnPc) only plays a minor role in stabilizing AlPc.

We now compare AlPc and ZnPc on a geometrical point of view. Given the larger stability of AlPc in the top site and the relatively minor difference between top and hollow sites for ZnPc, we focus on the top site for both species. In both cases the molecule preserve the flat structure of the macrocycle. We find that the aromatic ring sits at 3.19 Å (3.13 Å) from the outer Al layer for ZnPc (AlPc), with the central metal atom that sits at 2.89 Å (2.57 Å), hence more towards the surface. We remark that the adsorbed configuration of AlPc also exhibits a fourfold symmetry at the metal-N_4 center, at variance with that of the gas phase

molecule where the partial occupation of a degenerate orbital yields to D_{2h} geometry. This issue is discussed in a dedicated section below.

3.2. Electronic properties

We now discuss the electronic properties of the adsorbed molecules. In Fig. 2, we show the projected density of states of ZnPc and AlPc adsorbed at the top surface site of Al(100). There, we separate the orbital character according to π and σ symmetry.

The central metal atom contributes weakly to the DOS around the Fermi energy E_F. For ZnPc, we see a coupling of the HOMO -1 with σ symmetry to the $d_{x^2-y^2}$ Zn orbital, in agreement with the literature [3]. Contributions from Al can be seen only at energies lower than -5 eV. Coming to states from the macrocycle, slightly below -1 eV one recognizes the HOMO of Pc, and at small positive energies and twice as intense, the twofold LUMO. Focusing on the latter, this state appears right above the Fermi energy E_F, whereas it crosses E_F for AlPc, indicating that the unpaired electron due to the trivalent Al atom in AlPc is not fully transferred onto the substrate upon adsorption.

To mitigate the limitations of the semi-local PBE exchange correlation functional in describing the electronic properties, we have also computed the electronic DOS with the hybrid functional HSE [28,29]. We have considered ZnPc and AlPc adsorbed on a 5-layer slab and report the results in Fig. 2, overall confirming the results obtained by PBE considering the position of molecular orbitals with respect to the Fermi level. The change in energy for the molecule HOMO and LUMO is only minor; larger shifts are computed for more localized orbitals, such as σ states at deeper energies, where the treatment of self-interaction is more important.

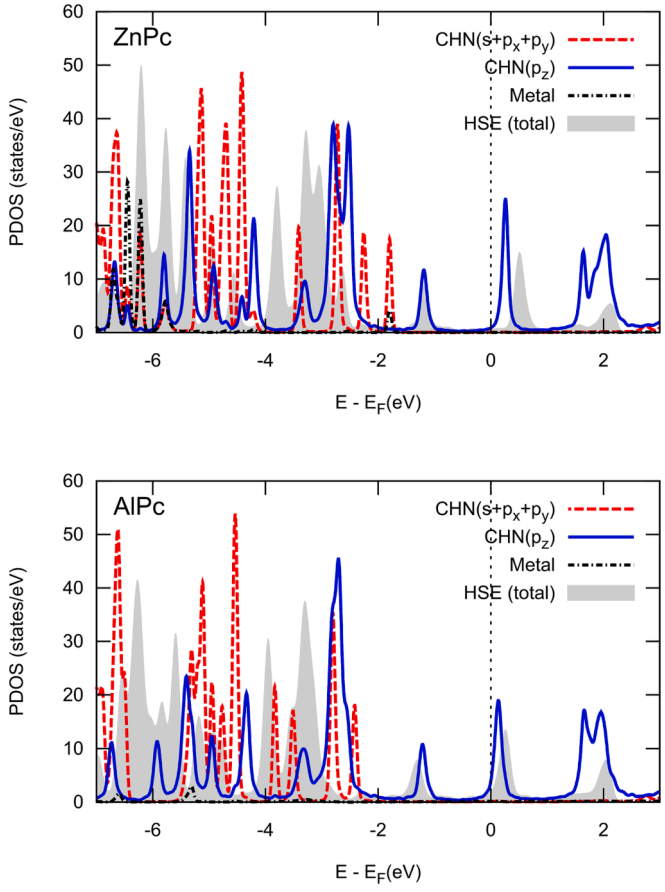

Fig. 2. Projected density of states of adsorbed ZnPc (top) and AlPc (bottom), computed with a 10-layers Al(100) slab. The gray shaded area is the corresponding results with the HSE functional (computed with a 5-layers slab).

The interaction of the molecules with the surface is well visualized by considering the displacement of electron density upon adsorption. For this purpose, in Fig. 3 we report the difference $\Delta\rho_{ads} = \rho_{mol/surf} - \rho_{mol} - \rho_{surf}$, where the molecule and surface electron densities have been computed at the same atomic coordinates as in the full system (hence, the LUMO is degenerate also for AlPc). For ZnPc, we observe in Fig. 3(a) a reduction of electron density from the pyrrolic N atoms as well as from the region between them and Zn, and an accumulation in the region between the Zn atom and the surface. By looking at the planar average of the electron density, computed as a function of the distance from the surface in Fig. 3(d), it can be clearly seen that on the average the main result is a polarization towards the surface of the electron density in the interface region. This reduces the surface electric dipole and the corresponding surface work function by 0.17 eV. Relatively small variations are seen in the Löwdin charges, -0.08 e overall for the four pyrrolic N atoms and -0.01 e for Zn, compensated by an increased density spread through C atoms leading to $+0.14$ e for the full molecule.

Moving to the case of AlPc reported in Fig. 3(b), a more pronounced modification can be observed: here, also the atoms surrounding the central Al atom contribute to displacing charge towards the surface. It is remarkable that their density depletion have approximately the shape of the LUMO orbital (summed over the two degenerate states that differ by a 90° rotation), showing the contribution by the unpaired electron due to the Al atom, occupying the LUMO in the gas phase molecule. In this case, the work function lowers by 0.22 eV. Here, Löwdin charge on the pyrrolic N atoms lowers by -0.17 e total, and that of the central Al increases by 0.25 e, the molecule overall having $+0.21$ e than in the gas phase.

It is then instructive to consider, as a comparison, a chloroaluminium phthalocyanine (ClAlPc) molecule in the gas phase. We can indeed think of this system as to a AlPc molecule bonded to a Cl atom, and perform the same analysis where the Cl atom plays the role of the "substrate". The corresponding $\Delta\rho_{ads}$ is shown in Fig. 3(c) and exhibits a remarkable similarity to the one of AlPc/Al(100). The planar average in Fig. 3(d) shows the same behaviour and in addition an increase of electron density around the Cl atom.

3.3. Magnetism and symmetry of AlPc

We recall that the unpaired electron in the free AlPc molecule occupies the LUMO of the Pc aromatic system, lifting its degeneracy and leading to a lowered D_{2h} symmetry [24], at variance with ZnPc. Nonetheless, the AlPc molecule is unstable in its free form so that synthesis by on-surface reactions may be adopted. Experiments have shown that the AlPc molecules may retain these free-form features when synthesized on Au(111) [24], while they are lost for isolated molecules on lead [25]. It is therefore interesting to deepen our discussion specifically on this point, for AlPc/Al(100). Indeed, the interaction with the surface [33], or with additional ligands [34], plays a crucial role to determine the magnetic configuration of adsorbed phthalocyanines, and in our specific case an interaction that is stronger on aluminium than on gold [22,35], is likely to enhance significantly the hybridization between the molecule and substrate states.

According to our calculations, the most stable adsorption configuration of AlPc exhibits an approximate fourfold symmetry in the metal-N_4 center alike for ZnPc. We have performed additional calculations to explore different possibilities. In particular, we initiate structural optimizations for adsorbed molecules with coordinates taken from gas phase D_{2h} molecules; notwithstanding, upon optimization a fourfold geometry was obtained.

We then considered the issue of orbital magnetization. Since this may interplay with the distortion, we have taken as initial structure one that is as close as possible to the adsorbed case, but retaining a twofold in-plane symmetry as in the free molecule. Namely, the in-plane xy coordinates are extracted from a free D_{2h} molecule and the z ones from the

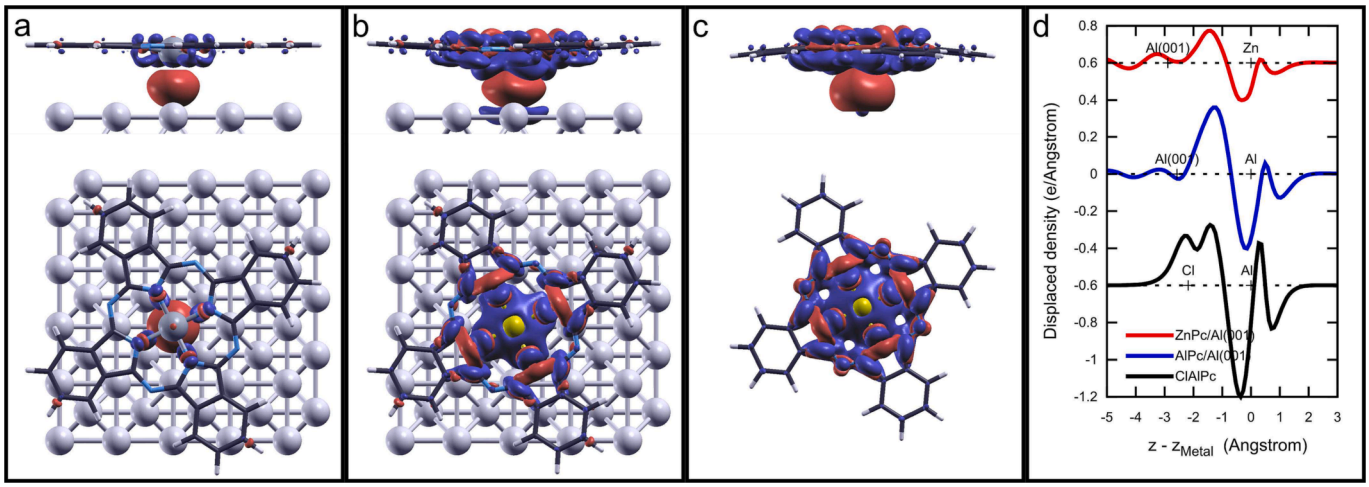

Fig. 3. Side and top view of electron density displacement upon adsorption of ZnPc (a) and AlPc (b) on Al(100). The bond charge of AlPc to a Cl atom is shown in panel (c). The chosen isovalue is 0.005 Å^{-3}. Red/blue surfaces correspond to electron accumulation/depletion. Panel (d): values of $\Delta\rho_{ads}$ integrated in a plane parallel to the surface and plotted as a function of its distance from the central metal atom along the surface normal z.

optimized on-surface structure. As a starting magnetic configuration, we selected one where the C and N atoms whose p_z orbitals take part to the LUMO state are assigned the same magnetization as in the free molecule. However, when this is placed on the surface, a non-magnetic solution was obtained. We verified that the same outcome is obtained upon reducing the smearing of electronic energy levels from 0.005 Ry to 0.001 Ry. We could enforce a magnetic solution by constraining the atomic magnetization as implemented in QuantumESPRESSO through Lagrange multipliers: also in this case, however, we found a small value of the spin polarization amounting to $\approx 0.25\ \mu_B$/molecule only, even with values of the multiplier $\lambda = 10$, i.e., ten times the default. A larger magnetization, with atomic values comparable to those of the free molecule, was obtained by choosing as target values for the atomic magnetization amounts that are unphysically 10 times larger. We hence conclude that the hybridization of molecular orbitals with Al(100) states destroys both magnetism and asymmetry of AlPc.

The adsorbate–substrate interaction and adsorbate electronic properties depend critically on the adsorption height, whose precise determination is notoriously difficult to determine given the relevant role of dispersion interactions [6]. Understanding the dependence of our results on this parameter is then important. Hence, we repeat the calculation for a AlPc molecule frozen in the twofold in-plane geometry described above, upon further displacing all its atoms away from the surface by the amount Δz. We report in Fig. 4 the resulting magnetization of the molecule as a function of Δz. According to DFT calculations, already a relatively small variation of height may induce a non-zero magnetization, but values approaching 1 μ_B are obtained only at fairly large distances. In all cases, although with different magnitude, magnetism occurs as a consequence of filling unevenly the unpaired LUMO, as testified by the magnetization density shown in the insets of Fig. 4 for two values of Δz.

4. Experimental results

Fig. 5a shows two Pc molecules imaged after deposition of ZnPc on Al (100) at room temperature. A white cross is superimposed over the molecules to indicate the crystallographic directions of Al(100), shown in the inset of Fig. 5a. In this way, it is possible to measure the azimuthal orientation of the molecules, which is defined as the angle between the lobe and the crystallographic directions of Al(100). The bottom molecule has an azimuthal angle ϕ of 24°, while for the top molecule $\phi = -30°$. Due to the square symmetry of both Pc and the Al(100) surface, these orientations are equivalent and in very good agreement with the one computed for Pc clusters in subsection adsorption configuration.

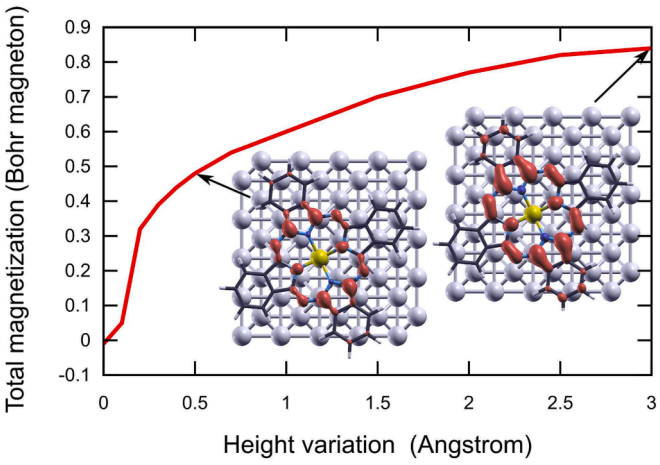

Fig. 4. Dependence of the total magnetization per cell of AlPc molecules rigidly lifted from Al(100). Insets report the magnetization density (spin-majority – spin-minority electron density) for $\Delta z = 0.5$ Å and $\Delta z = 3.0$ Å.

Therefore, molecules spontaneously adsorb with the correct angle to form clusters.

The sample is then annealed at 160 °C to diffuse the zinc atoms into the crystal [23] and exclude the on-surface presence of zinc atoms. STM characterization performed after annealing shows no evidence for structural/morphological changes occuring in Pc molecules. The STM image of an isolated Pc molecule on Al(100) after sample heating, Fig. 5b, shows that the molecule adsorbs flat and parallel to the surface. Specifically, the line profile shown in Fig. 5c clearly indicates the absence of a central depression. Since the simulated STM image of the distorted ·Pc visibly displays a central depression (see Fig. 1d), we can exclude the presence of this configuration, in agreement with the calculated energetics. Since the presence of H_2Pc has been excluded by N 1s XPS data [23], Fig. 5b shows the typical morphology of a metal-phthalocyanine, as it was simulated for the on-surface synthesized AlPc (Fig. 1c).

5. Discussion

XPS results indicate that after the ZnPc growth at 160 °C there are no zinc atoms on the surface [23], therefore the only remaining possibility able to explain all the experimental results is the synthesis of AlPc after

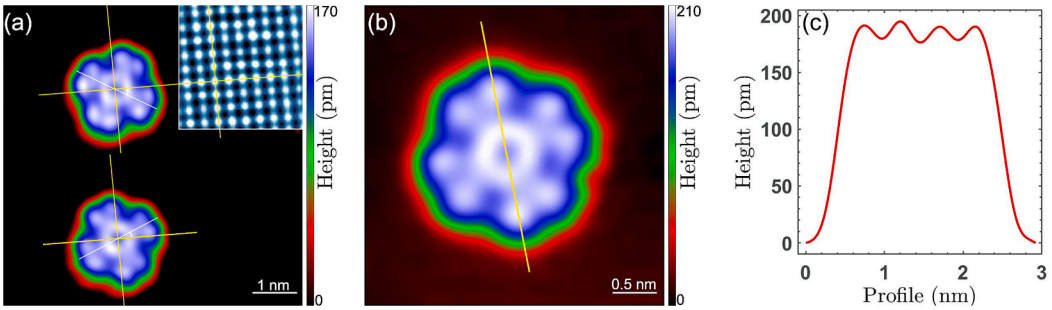

Fig. 5. STM topography of AlPc obtained by transmetalation of ZnPc deposited on Al(100) at room temperature; (a) STM image obtained immediately after deposition (V = −1.0 V, I = 1 nA). Over the molecules the crystallographic directions of Al(100) are superimposed. The figure inset shows the clean Al(100) lattice (b) STM image obtained after annealing to 160 °C (V = −0.35 V, I = 50 pA). The yellow line superimposed corresponds to the line profile reported in (c).

the loss of the zinc atom and the capture of an Al atom from the substrate. Indeed, as already noted, molecules deposited at room temperature show the same morphology of those imaged after annealing to 160 °C (compare, respectively, Figs. 5a and 5b). Furthermore, the room temperature Zn $2p_{3/2}$ XPS data show only one asymmetric peak with a significant shift with respect to the bulk phase, indicating that all the zinc atoms are metallic [23]. Therefore, our experimental data indicate that even at room temperature the transmetalation occurs and the deposited ZnPcs became AlPcs. Our DFT calculations confirm the transmetalation of ZnPc on Al(100): the synthesis of AlPc is much more energetically favorable than the adsorption of ZnPc, since 2 eV per molecules are released in the transmetalation process, see Table 2, and the inclusion of Al into a demetallated phthalocyanine happens without any energy barrier.

This differs from what occurs for CoPc on Cu(111), where at room temperature two different cobalt peaks are observed, corresponding to metallic cobalt and cobalt bound to Pc [17]. The different amount of transmetalation at room temperature in the case of Al substrate (complete) and Cu substrate (partial) could be related to the valence of the metal substrate. We believe that a configuration featuring a trivalent atom within the phthalocyanine (Al) could be more favorable than one with a divalent atom (Zn or Cu). This is because the latter cannot establish a bond with the substrate through the central atom unless it changes its own electronic configuration.

Since the bond between AlPc and Al(100) is similar to the one between AlPc and a Cl atom, the magnetic character and symmetry of isolated AlPc could be lost on Al(100). Indeed, ClAlPc is a diamagnetic molecule with C_{4v} symmetry, while AlPc is paramagnetic with $D_{2\ h}$ symmetry [24]. In transition-metal Pc, the bonding with the Pc ring involves the two valence electrons of the central atom and the magnetic character, if present, derives from central atom's 3d electrons. Instead, the magnetic character of AlPc has a different origin. Since there are 3 aluminium valence electrons, two take part to the bond with the Pc ring, while the third, which we call extra electron, occupies one of the two degenerate LUMO levels [24]. In the case of ClAlPc, the extra electron takes part to the bond with Cl and it does not fill the LUMO [36]. As the isolated ClAlPc molecule is a closed-shell structure, it exhibits diamagnetic properties [37]. Fig. 3 illustrates that, even in the case of AlPc/Al(100), the additional electron participates in a bond, in this case with the substrate. Moreover, as we computed, there are no electrons from the central atom in the LUMO, see Fig. 2.

Then, considering the similarities between ClAlPc and AlPc/Al(100) it is not surprising that also for AlPc/Al(100) there is no magnetic moment. As it can be seen in Fig. 4, the restoration of the magnetic moment occurs only when the interaction between the substrate and the molecule is eliminated by placing the molecule far away from the substrate, effectively isolating it. This allows the extra electron to occupy the LUMO orbital.

The previous experiment of on-surface synthesis of AlPc on gold [24] indicates that isolated molecules are paramagnetic as a consequence of the filling of the LUMO with the extra electron. AlPc/Au(111) electronic structure is different from the one observed on Al(100), where we have computed that the extra electron does not fill the LUMO.

This different bond could be related to the interface interaction. Indeed, aluminium and gold have fundamentally distinct electronic structures. Al has outer electrons that can be closely approximated as nearly-free, whereas Au exhibits a high concentration of well-localized d electrons. The different electronic structure results in a distinct interaction at the interface. Indeed CuPcs on Al(100) are chemisorbed with a charge transfer from the substrate to the molecule LUMO [22]. Instead, on gold they have the occupied orbitals hybridized with the substrate [35], but no charge transfer to the LUMO level is observed [9,35]. The different interaction is such that even the bulk growth is affected [21]. In this framework it is not surprising that also the AlPc has a different interaction with these two substrates and, consequently, a possible different magnetism.

6. Conclusion

ZnPc molecules adsorbed on Al(100) spontaneously transmetalate forming the air unstable AlPc. The removal of Zn atoms is accompanied by the insertion of a surface Al atom, which for an hypothetical demetalated molecule occurs without any barrier. Overall, this process is related to the formation of a bond between the AlPc and the substrate, which stabilises the molecule and resembles the one between Cl and Al in ClAlPc. For this reason, the extra electron does not fill the LUMO. The symmetry and magnetism of isolated AlPc are modified by the bonding of the molecule with the substrate. This is in contrast to AlPc/Au(111), where symmetry and magnetism are maintained. We attribute this difference to the distinct interactions between the molecule and the two substrates [22,23,35].

Declaration of generative AI and AI-assisted technologies in the writing process

During the preparation of this work D.P. used openAI/chatGPT in order to improve readability and language. After using this tool, the author reviewed and edited the content as needed and takes full responsibility for the content of the publication.

Declaration of Competing Interest

The authors declare that they have no known competing financial interests or personal relationships that could have appeared to influence the work reported in this paper.

Data availability

Data will be made available on request.

Acknowledgment

G.F. gratefully acknowledge Giuseppe Mattioli and Matteo Cococcioni for fruitful discussions. We acknowledge the CINECA award under the ISCRA initiative, for the availability of high performance computing resources and support. D.C. and G.K. acknowledge partial financial support from the Slovenian Research Agency (research program P1-0112 and research projects J1-3007 and J2-2514).

Appendix A. Supplementary data

Supplementary data associated with this article can be found, in the online version, at https://doi.org/10.1016/j.ica.2023.121790.

References

[1] Rosemary R. Cranston, Benoît H. Lessard, Metal phthalocyanines: Thin-film formation, microstructure, and physical properties, RSC Adv. 11 (35) (2021) 21716–21737.
[2] Nicolas Papageorgiou, Eric Salomon, Thierry Angot, Jean-Marc Layet, Luca Giovanelli, Guy Le Lay, Physics of ultra-thin phthalocyanine films on semiconductors, Prog. Surf. Sci. 77 (5–8) (January 2004) 139–170.
[3] Meng-Sheng Liao, Steve Scheiner, Electronic structure and bonding in metal phthalocyanines, metal=Fe Co, Ni, Cu, Zn, Mg. J. Chem. Phys. 114 (22) (Jun 2001) 9780–9791.
[4] Y.Y. Zhang, S.X. Du, H.-J. Gao, Binding configuration, electronic structure, and magnetic properties of metal phthalocyanines on a Au(111) surface studied with ab initio calculations, Phys. Rev. B 84 (Sep 2011), 125446.
[5] Jeremy Sanders, Nick Bampos, Zoe Clyde-Watson, Scott Darling, Joanne Hawley, Hee-Joon Kim, Chi Mak, Simon Webb, Axial coordination chemistry of metalloporphyrins, Cheminform 34 (2003) 11.
[6] Antoni Franco-Cañellas, Steffen Duhm, Alexander Gerlach, Frank Schreiber, Binding and electronic level alignment of π)conjugated systems on metals, Rep. Prog. Phys. 83 (6) (Jun 2020), 066501.
[7] Daniele Paoloni, Alessandro Ruocco, Cu-phthalocyanine long-range ordered bulk growth due to the weak interaction with highly oriented pyrolytic graphite substrate, Surf. Sci. 735 (2023), 122322.
[8] Cristina Isvoranu, John Åhlund, Bin Wang, Evren Ataman, Nils Mårtensson, Carla Puglia, Jesper N. Andersen, Marie-Laure Bocquet, Joachim Schnadt, Electron spectroscopy study of the initial stages of iron phthalocyanine growth on highly oriented pyrolitic graphite, J. Chem. Phys. 131 (21) (December 2009), 214709.
[9] Patrizia Borghetti, Afaf El-Sayed, Elizabeth Goiri, Celia Rogero, Jorge Lobo-Checa, Luca Floreano, Jose Enrique Ortega, Dimas G. de Oteyza, Spectroscopic Fingerprints of Work-Function-Controlled Phthalocyanine Charging on Metal Surfaces, ACS Nano 8 (12) (December 2014) 12786–12795.
[10] J. Michael Gottfried, Surface chemistry of porphyrins and phthalocyanines, Surf. Sci. Rep. 70 (3) (2015) 259–379.
[11] Can-Li Song, Yi-Lin Wang, Yan-Xiao Ning, Jin-Feng Jia, Xi Chen, Bo Sun, Ping Zhang, Qi-Kun Xue, Xucun Ma, Tailoring phthalocyanine metalation reaction by quantum size effect, J. Am. Chem. Soc. 132 (5) (2010) 1456–1457. PMID:20078042.
[12] Yun Bai, Florian Buchner, Matthew T. Wendahl, Ina Kellner, Andreas Bayer, Hans-Peter Steinrück, Hubertus Marbach, J. Michael Gottfried, Direct metalation of a phthalocyanine monolayer on Ag(111) with coadsorbed iron atoms, J. Phys. Chem. C 112 (15) (2008) 6087–6092.
[13] Alexander Sperl, Jörg Kröger, Richard Berndt, Controlled Metalation of a Single Adsorbed Phthalocyanine, Angewandte Chemie International Edition 50 (23) (2011) 5294–5297.
[14] Alexander Sperl, Jörg Kröger, Richard Berndt, Demetalation of a single organometallic complex, J. Am. Chem. Soc. 133 (29) (2011) 11007–11009. PMID:21702473.
[15] Lars Smykalla, Pavel Shukrynau, Dietrich R.T. Zahn, Michael Hietschold, Self-Metalation of Phthalocyanine Molecules with Silver Surface Atoms by Adsorption on Ag(110), J. Phys. Chem. C 119 (30) (2015) 17228–17234.
[16] Min Chen, Michael Röckert, Jie Xiao, Hans-Jörg Drescher, Hans-Peter Steinrück, Ole Lytken, J. Michael Gottfried, Coordination reactions and layer exchange processes at a buried metal–organic interface, J. Phys. Chem. C 118 (16) (2014) 8501–8507.
[17] Kongchao Shen, Bai Narsu, Gengwu Ji, Haoliang Sun, Hu. Jinbang, Zhaofeng Liang, Xingyu Gao, Haiyang Li, Zheshen Li, Bo Song, Zheng Jiang, Han Huang, Justin W. Wells, Fei Song, On-surface manipulation of atom substitution between cobalt phthalocyanine and the Cu(111) substrate, RSC Adv. 7 (2017) 13827–13835.
[18] Jan Herritsch, Stefan R Kachel, Qitang Fan, Mark Hutter, Lukas J Heuplick, Florian Münster, J. Michael Gottfried, On-surface porphyrin transmetalation with Pb/Cu redox exchange, Nanoscale 13 (31) (2021) 13241–13248.
[19] Catherine M. Doyle, John P. Cunniffe, Sergey A. Krasnikov, Alexei B. Preobrajenski, Zheshen Li, Natalia N. Sergeeva, Mathias O. Senge, Attilio A. Cafolla, Ni-Cu ion exchange observed for Ni(ii)-porphyrins on Cu(111), Chem. Commun. 50 (2014) 3447–3449.
[20] Katharina Diller, Anthoula C. Papageorgiou, Florian Klappenberger, Francesco Allegretti, Johannes V. Barth, Willi Auwärter, In vacuo interfacial tetrapyrrole metallation, Chem. Soc. Rev. 45 (2016) 1629–1656.
[21] Gian Marco Pierantozzi, Marco Sbroscia, Alessandro Ruocco, Templating effect of the substrate on the structure of Cu-phthalocyanine thin film, Surf. Sci. 669 (March 2018) 176–182.
[22] A. Ruocco, F. Evangelista, R. Gotter, A. Attili, G. Stefani, Evidence of charge transfer at the Cu-phthalocyanine/Al(100) interface, J. Phys. Chem. C 112 (6) (2008) 2016–2025.
[23] Daniele Paoloni, Gianluca Di Filippo, Dean Cvetko, Gregor Kladnik, Alberto Morgante, Alessandro Ruocco, Strong Chemical Interaction and Self-Demetalation of Zinc-Phthalocyanine on Al(100), J. Phys. Chem. C 124 (41) (October 2020) 22550–22558.
[24] I-Po Hong, Na Li, Ya-Jie Zhang, Hao Wang, Huan-Jun Song, Mei-Lin Bai, Xiong Zhou, Jian-Long Li, Gao-Chen Gu, Xue Zhang, et al., Vacuum synthesis of magnetic aluminum phthalocyanine on Au(111), Chem. Commun. 52 (68) (2016) 10338–10341.
[25] Chao Li, Jan Homberg, Alexander Weismann, Richard Berndt, On-surface synthesis and spectroscopy of aluminum phthalocyanine on superconducting lead, ACS Nano 16 (10) (2022) 16987–16995. PMID:36153959.
[26] John P. Perdew, Kieron Burke, Matthias Ernzerhof, Generalized gradient approximation made simple, Phys. Rev. Lett. 77 (18) (1996) 3865.
[27] Stefan Grimme, Jens Antony, Stephan Ehrlich, Helge Krieg, A consistent and accurate ab initio parametrization of density functional dispersion correction (DFT-D) for the 94 elements H-Pu, J. Chem. Phys. 132 (15) (Apr 2010), 154104.
[28] Jochen Heyd, Gustavo E. Scuseria, Matthias Ernzerhof, Hybrid functionals based on a screened Coulomb potential, J. Chem. Phys. 118 (18) (Apr 2003) 8207–8215.
[29] Jochen Heyd, Gustavo E. Scuseria, Matthias Ernzerhof, Erratum: “Hybrid functionals based on a screened Coulomb potential” [j. chem. phys. 118, 8207 (2003)], J. Chem. Phys. 124 (21) (Jun 2006), 219906.
[30] Paolo Giannozzi, Stefano Baroni, Nicola Bonini, Matteo Calandra, Roberto Car, Carlo Cavazzoni, Davide Ceresoli, Guido L Chiarotti, Matteo Cococcioni, Ismaila Dabo, et al., QUANTUM ESPRESSO: a modular and open-source software project for quantum simulations of materials, J. Phys.: Condens. Matter 21 (39) (Sep 2009), 395502.
[31] P. Giannozzi, O. Andreussi, T. Brumme, O. Bunau, M. Buongiorno Nardelli, M. Calandra, R. Car, C. Cavazzoni, D. Ceresoli, M. Cococcioni, et al., Advanced capabilities for materials modelling with Quantum ESPRESSO, J. Phys.: Condens. Matter 29 (46) (Oct 2017), 465901.
[32] Andrea Dal Corso, Pseudopotentials periodic table: From H to Pu, Comput. Mater. Sci. 95 (2014) 337–350.
[33] Elisabeth Wruss, Georgia Prokopiou, Leeor Kronik, Egbert Zojer, Oliver T. Hofmann, David A. Egger, Magnetic configurations of open-shell molecules on metals: The case of CuPc and CoPc on silver, Phys. Rev. Mater. 3 (8) (Aug 2019), 086002.
[34] Henning Maximilian Sturmeit, Iulia Cojocariu, Andreas Windischbacher, Peter Puschnig, Cinthia Piamonteze, Matteo Jugovac, Alessandro Sala, Cristina Africh, Giovanni Comelli, Albano Cossaro, et al., Room-temperature on-spin-switching and tuning in a porphyrin-based multifunctional interface, Small 17 (50) (2021) 2104779.
[35] F. Evangelista, A. Ruocco, R. Gotter, A. Cossaro, L. Floreano, A. Morgante, F. Crispoldi, M.G. Betti, C. Mariani, Electronic states of CuPc chains on the Au(110) surface, J. Chem. Phys. 131 (17) (2009), 174710.
[36] S. Kera, H. Yamane, H. Honda, H. Fukagawa, K.K. Okudaira, N. Ueno, Photoelectron fine structures of uppermost valence band for well-characterized ClAl-phthalocyanine ultrathin film: UPS and MAES study, Surf. Sci. 566–568 (2004) 571–578. Proceedings of the 22nd European Conference on Surface Science.
[37] Gregory P. Eyer, Kevin R. Kittilstved, Trisha L. Andrew, Anomalous paramagnetism in closed-shell molecular semiconductors, J. Phys. Chem. C 121 (45) (2017) 24929–24935.

Supplementary material for: Spontaneous transmetalation at the ZnPc/Al(100) interface

Guido Fratesi[a], Daniele Paoloni[b], Luca Persichetti[c], Luca Camilli[c], Antonio Caporale[c], Anu Baby[d,e], Dean Cvetko[f,g,h], Gregor Kladnik[f,h], Alberto Morgante[h,i], Alessandro Ruocco[b],

[a]*Physics Department "Aldo Pontremoli" University of Milan, 20133, Italy*
[b]*Dipartimento di scienze, Università degli studi Roma Tre, Via della Vasca Navale 84, 00146 Rome, Italy*
[c]*Dipartimento di Fisica, Università di Roma "Tor Vergata", Via Della Ricerca Scientifica, 1-00133 Rome, Italy*
[d]*Department of Materials Science, University of Milano-Bicocca, 20125 Milano, Italy*
[e]*Now at: STMicroelectronics, Via Tolomeo 1, 20010 Cornaredo, Italy.*
[f]*University of Ljubljana, Faculty of Mathematics and Physics, Ljubljana SI-1000, Slovenia*
[g]*Institute J. Stefan, Ljubljana SI-1000, Slovenia*
[h]*Laboratorio TASC CNR-IOM, Trieste 34127, Italy*
[i]*Physics Department, University of Trieste, Trieste 34127, Italy*

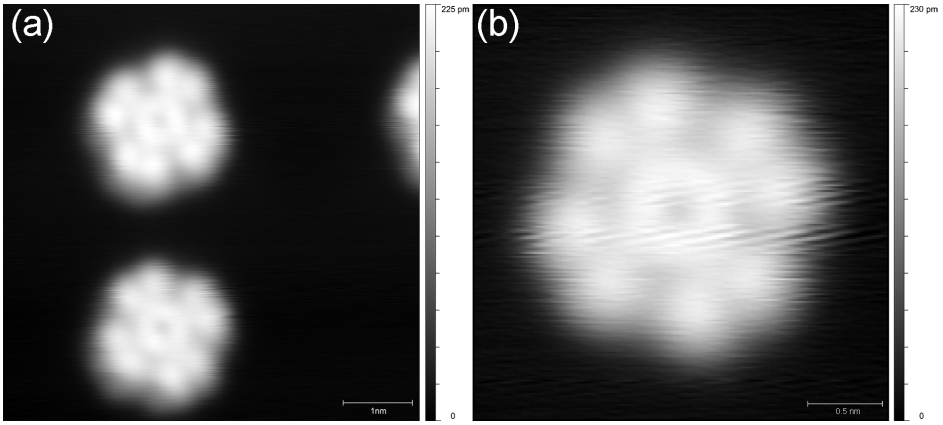

Figure S1: Unfiltered version of STM images contained in figure 5. (a) STM image obtained immediately after deposition (V=-1.0 V, I=1 nA). Over the molecules the crystallographic directions of Al(100) are superimposed. The figure inset shows the clean Al(100) lattice (b) STM image obtained after annealing to 160 °C (V=-0.35 V, I=50 pA).

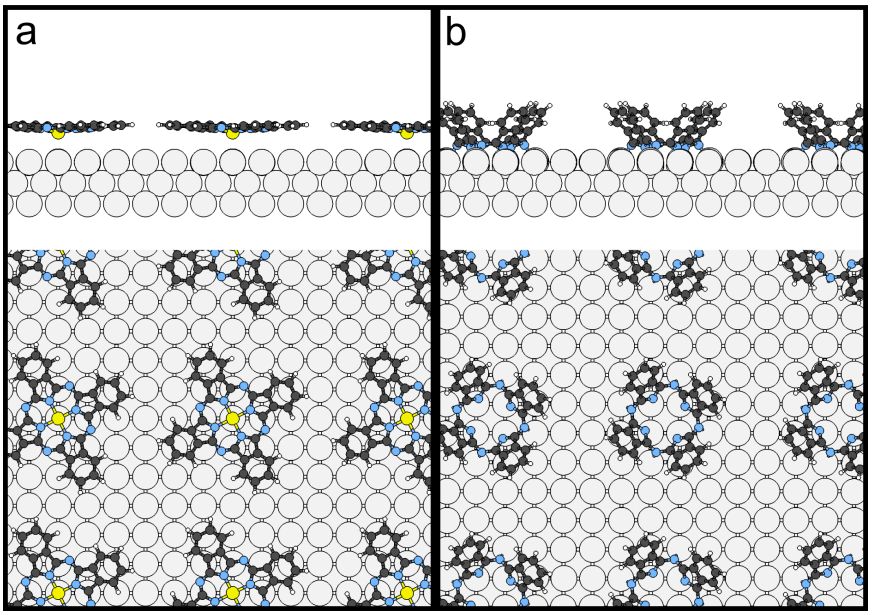

Figure S2: Same as Fig. 1 in the main manuscript, but optimized in a larger 6×6 unit cell. The obtained configurations are nearly indistinguishable from those of the 5×5 unit cell, testifying that the molecular packing is not responsible for the distortion of ·Pc. The norm of displacement vector upon changing from the small to the large cell, $\sqrt{\sum_I |\mathbf{R}_I - \mathbf{R}'_I|^2}$ where $\mathbf{R}_I$ and $\mathbf{R}'_I$ are atomic coordinates in the two cells, amounts to only 0.03 Å in both AlPc and ·Pc cases.